Density-functional study of CO adsorbed on Rh_N (N = 2–19) clusters*

Tian Fu-Yang(田付阳)† and Shen Jiang(申 江)

Institute for Applied Physics, University of Science and Technology Beijing, Beijing 100083, *China*

(Received 31 March 2011; revised manuscript received 3 June 2011)

We investigate the structural, electronic and adsorption properties of one single CO molecule adsorbed on Rh_N (N = 2–19) clusters, using the density-functional theory in the spin-polarized generalized gradient approximation. It is found that the structural growth model of the Rh_N clusters transforms from double layers (N = 12–16) to three layers (N = 17–19). Three different adsorption types are the atop site adsorption for N = 6, 8, 9, 11, 12, the bridge site adsorption for N = 2–5, 7, 10, 13–15, 17 and the face adsorption for N = 16, 18, 19. The adsorption abilities of Rh_N clusters are related to C–O bond length, vibrational frequency, adsorption energy and the charge transfer between CO and Rh clusters as well as the electronic density of state. With the increase of Rh cluster size, the adsorption energy of CO adsorbed on Rh_N clusters tends to be 2.2 eV–2.3 eV, which is 0.2 eV–0.3 eV larger than the theoretical value (about 2.0 eV) of CO molecule adsorption on clean Rh (111) surface.

Keywords: CO–Rh_N compounds, adsorption energy, vibrational frequency, electronic density of state

PACS: 31.10.+z, 31.15 ae, 31.15.E– **DOI:** 10.1088/1674-1056/20/12/123101

1. Introduction

The catalytic activity of transition metal (TM) clusters has been widely investigated. The interaction of one CO molecule with partial TM clusters in the gas-phase environment by vibrational spectroscopy have been systemically studied by Fielicke *et al.*[1–4] Based on the density functional theory (DFT), the absorption characters of CO molecules absorptions on TM clusters have been investigated.[5–9]

It is well known that rhodium metal is one of the best catalysts for the removal of carbon monoxide and nitric oxide from auto exhaust gases. Thus, interest in CO molecule adsorption on Rh clusters can be traced back to many years ago. Early studies were concerned mainly with the geometries and electronic properties as well as vibrational frequencies of the $Rh(CO)_n$ compounds. Based on the infrared spectrum experiments and DFT calculations, Zhou and Andrews[10,11] reported on the neutral and the charged CO–Rh complexes. The interactions of CO molecules with small Rh clusters have been studied.[12,13] The CO bonding behaviours in formation of $Rh_x(CO)_y$ ($x \leq 4$, $y \leq 2$) have also been investigated on the basis of the molecular orbital and the natural bond order analysis.[12] A series of saturated cationic rhodium carbonyl complexes $Rh_n(CO)_m{}^+$ (n = 1–6) was structurally characterized by infrared multiple photon dissociation (IR-MPD) spectroscopy.[13] Fielicke *et al.*[14,15] investigated the vibrational spectroscopy of gas-phase CO–Rh complexes using the IR-MPD spectroscopy and found that the IR absorption spectra of neutral and charged Rh_nCO (n = 3–15) complexes were between 1650 cm^{-1} and 2200 cm^{-1} in the frequency range of v(CO). To our knowledge, there are a few theoretical studies dealing with the interaction of a single CO molecule with rhodium clusters containing more than four metal atoms so far.

In addition, the structural and electronic properties of Rh clusters have been widely studied by using experimental and theoretical methods.[16–34] However, some DFT calculations were inconsistent with each other. The differences in ground-state structure and in electronic property are mainly due to the range of initial configuration considered for each cluster size or different details of the calculations. In addition, partly filled d orbitals of TM element result in a number of alternative low-lying isomers within the very narrow energy range for TM clusters.

In this work, we focus mainly on (i) the ground-state structures and the structural growth model of bare Rh clusters, (ii) the adsorption characteristic of

*Project supported by the National Basic Research Program of China (Grant No. 2011CB606401).

†Corresponding author. E-mail: fuytian@gmail.com

© 2011 Chinese Physical Society and IOP Publishing Ltd

single CO on Rh clusters, (iii) the influence of structural and electronic properties by CO adsorption for Rh clusters and comparison of the free CO molecule with the CO adsorbed on Rh clusters. In Section 2, we describe the computational method and parameters. In Section 3, we present the results and discussion. Conclusions are given in the last section.

2. Computational details

In order to search for the ground-state structures of bare Rh_N (N = 2–19) clusters, the initial configurations are obtained by optimizing independent geometries and referring to previous calculation results.[21−33] During choosing initial configurations of CO–Rh_N complexes, the low-lying isomers of bare Rh clusters were considered as the reactants of CO at various possible adsorption sites, including the atop, bridge and hollow sites. Then the adsorption structures are optimized without any symmetry constraints. Finally, the configuration with the lowest energy is taken as the lowest-energy structure. For each size, the local minimum of the potential energy surface is guaranteed by the harmonic vibrational frequency without the imaginary mode.

All calculations were performed using the DFT provided by the DMoL package.[35] The density functional is treated with the general gradient approximation(GGA) corrected-exchange potential of the Perdew–Burke–Ernzerhof (PBE).[36] We chose the DFT-based relativistic semi-core pseudopotential (DSPP)[37] and double numerical basis set in a d-polarization function (DND). The spin-unrestricted consistent field calculations were performed with a convergence criterion of 10^{-5} a.u. on the total energy and electron density. The convergence criteria were set to be 0.005 Å (1 Å=0.1 nm) for the displacement, 0.004 Hartree/Å (1 Hartree=27.21 eV) for the force parameter on the atoms, and 2×10^{-5} Hartree for the energy change in the geometry optimization.

The accuracy of the current computational scheme was evaluated by the calculations of CO molecule and Rh_2 dimer. For a free CO molecule, the bond length 1.143 Å, binding energy 11.6 eV and vibrational frequency 2126.2 cm^{-1} are all in accordance with the corresponding experimental values (1.128 Å, 11.2 eV, and 2143.2 cm^{-1}).[38,39] The vibrational frequency of CO molecule is 2101.4 cm^{-1} with the BLYP/DNP/DSPP method and is 2098.7 cm^{-1} with the HCTH/DNP/DSPP method. As for the Rh_2 dimer, previous theoretical and experimental values showed a quintet state to be the ground state with a bond length about 2.30 Å[40] and a stretching frequency of 283 cm^{-1},[17] our present way predicts that the bond length is 2.35 Å and the stretching frequency is 246 cm^{-1} for the Rh_2 dimer with a quintet state. Such a test indicates that the PBE/DND/DSPP approach is reliable and sufficient to the system.

3. Results and discussion

In this section, we discuss the geometies and the relative stabilities of bare Rh clusters. The properties of CO–Rh_N (N = 2–19) complexes are investigated, including the ground-state structures, C–O vibrational frequencies, adsorption energies and charge transfer distributions as well as electronic densities of state.

3.1. Structure and stability

The ground-state structures of bare Rh_N clusters and of CO–Rh_N compounds are shown in Figs. 1 and 3, respectively. There are three different adsorption types for CO–Rh_N compounds: the atop site for N = 6, 8, 9, 11, 12, in which the C atom sits on an Rh atom, the bridge site for N = 2–5, 7, 10, 13–15, 17, in which the C atom sits over the Rh–Rh bond, and the face site for N = 16, 18, 19, in which the C atom sits on the Rh–Rh–Rh triangular plane. The relative stabilities of bare Rh clusters are displayed in Fig. 2 based on the average binding energy per atom (E_b) and the second-order energy difference (Δ^2E).

3.1.1. Ground-state structure and relative stability for bare Rh cluster

For the ground-state structures of bare Rh_N clusters, the basic units are composed mainly of triangles and quadrangles. The tetrahedron with T_d symmetry is viewed as the lowest-energy structure of Rh_4 cluster, which is accumulated by four regular triangles. The ground-state structure of Rh_5 looks like a square-based pyramid with C_{4v} symmetry, including four triangles and one square. The octahedron and caped antiprism are regarded as the lowest-energy structures of Rh_6 and Rh_7 clusters, respectively. The ground state structure of Rh_8 cluster is cubic, which is in good agreement with that previously reported.[25−27] The triangle-layer structure, 60° difference between any two parallel layers, is regarded as the ground-state structure of Rh_9. One Rh dimer parallelly sits on the

face of cubic. The configuration, which looks like a house, is viewed as the ground-state structure of Rh_{10} cluster with C_{2v} symmetry. Although the number of different faces in Rh_{10} is up to 5, the configuration with slope roofing capped is viewed as the ground-state structure of Rh_{11} and has C_s symmetry.

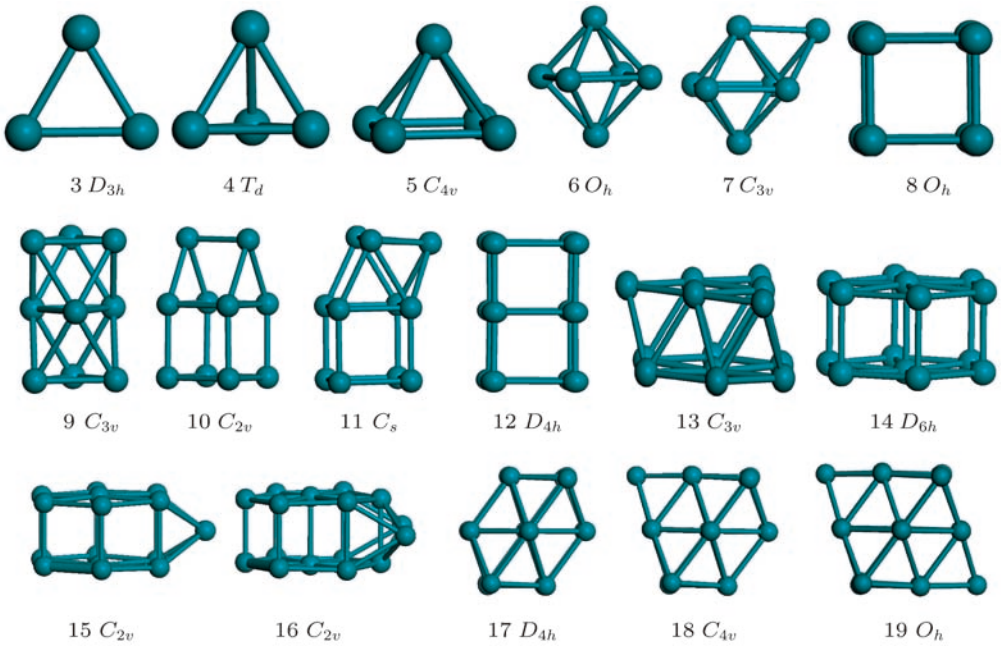


Fig. 1. (colour online) Ground-state structures of bare Rh_N (N = 2–19) clusters.

With the increase of cluster size, the growth model of ground-state structure transforms from double layers to three layers for N = 12–19. As shown in Fig. 1, the lowest-energy geometry of Rh_{12} is D_{4h} symmetry, in which two cubes couple together with one co-surface. The cluster with 13 atoms is particularly interesting. In previous works, different configurations have been reported as the ground-state structure of Rh_{13} cluster, including icosahedron, caped double cubes, hexagonal closely packed and body-centred cubic.[28–33] The disagreement may be due to different exchange–correction functionals employed. In our calculations, the ground-state structure of Rh_{13} with double layers consisted of a face-centred hexagon and a triangle including six atoms. Two overlapped hexagons with one central atom are seen as the ground-state structure of Rh_{14} cluster. One Rh atom capped on the quadrilateral of the double hexagons is viewed as the-lowest energy structure of Rh_{15}. The ground-state structure of Rh_{16} is seen as the configuration of Rh_{14} capped on two neighbouring quadrilateral by double Rh atoms. The lowest-energy structure of Rh_{17} is viewed as a three-layer geometry with D_{4h} symmetry, which is composed of twenty-four triangles and two squares. For Rh_{18} or Rh_{19}, the ground-state structure is viewed as one or two Rh atoms capped on one or double squares of Rh_{17}. The symmetry is C_{4v} for Rh_{18} and O_h for Rh_{19}. Each face of the ground-state structure of Rh_{19} has a triangle shape, which is seen as finitely perfect surface of Rh (111) plane family.

For the relative stability of bare Rh clusters, we calculated the E_b and $\triangle^2 E$. They are defined as:

$$E_b = [NE(\mathrm{Rh}) - E(\mathrm{Rh}_N)]/N, \quad (1)$$

$$\Delta^2 E(\mathrm{Rh}_N) = E(\mathrm{Rh}_{N+1}) + E(\mathrm{Rh}_{N-1}) - 2E(\mathrm{Rh}_N), \quad (2)$$

where $E(*)$ values represent the energies of the corresponding to Rh_N, Rh_{N-1}, and Rh_{N+1} clusters as well as Rh atom. The E_b shown in Fig. 2 increases monotonically with the increase of total number of atoms in bare Rh clusters. For N = 2–8, the E_b increases rapidly from 1.2 eV/atom for the dimer to 3.0 eV/atom for the cube. In the range N = 9–19, the E_b increases gradually. The $\triangle^2 E$ is a sensitive quantity that reflects the relative stability of the investigated clusters. As illustrated in Fig. 2, the relative stability of bare Rh cluster displays the odd–even oscillation.

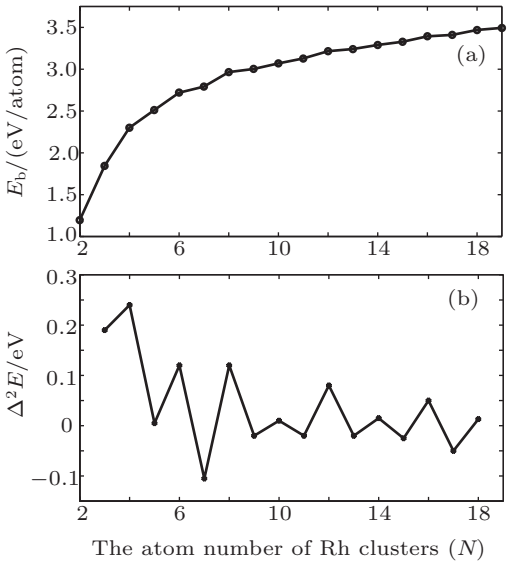


Fig. 2. The values of E_b of bare Rh_N (N = 2–19) clusters (a) and the Δ^2E of the Rh_N (N = 2–19) clusters (b) each as a function of cluster size.

3.1.2. Structural properties for CO–Rh_N compounds

For atop site adsorption, different sites are all considered according to the symmetry of bare Rh cluster. The CO molecule prefers to be adsorbed on Rh atom with low coordination number and has less effect on the structure of bare Rh cluster. In the case of Rh_8 cluster, the length of Rh–Rh bond is about 2.455 Å, but the corresponding bond length between Rh neighbouring to C and its three neighbouring Rh atoms is about 2.488 Å. The adsorption energy of bare Rh_N cluster with high symmetry is smaller than that of bare Rh_N cluster with low symmetry. For example, the energy adsorption of the bare Rh_8 with O_h symmetry is 2.195 eV, while the value of Rh_{11} with C_s symmetry is 2.343 eV.

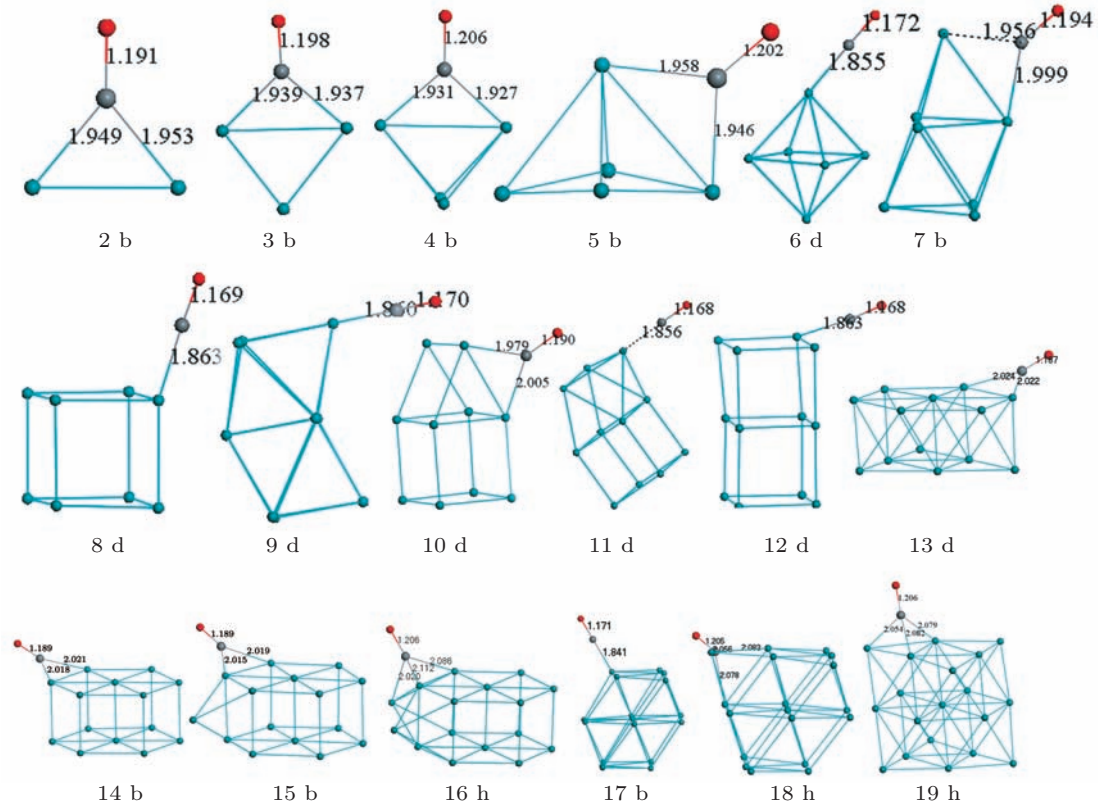


Fig. 3. (colour online) Lowest-energy geometries of CO–Rh_N compounds, with symbols 'd', 'b' and 'h' representing atop site adsorption, bridge site adsorption and face site adsorption, respectively.

The bridge site adsorption dominates between CO molecule and bare Rh_N (N = 2–19) clusters. The length of the Rh–Rh bond of absorbed CO molecule is elongated compared with the corresponding Rh–Rh bond length of bare Rh cluster. The Rh–Rh bond length is 2.354 Å for bare Rh_2 dimer, but the corresponding value is 2.468 Å in the CO–Rh_2 compound. The length of Rh–Rh bond adsorbed CO molecule is 2.639 Å in the CO–Rh_{14} compound, while the corresponding Rh–Rh bond length is 2.603 Å in bare Rh_{14} cluster. It is seen in Fig. 3 that two C–Rh bonds are not consistent with each other. In Fig. 4, the

variational length of Rh–Rh bond of adsorbed CO molecule is displayed for the bridge site adsorption. The CO molecule lengthens the Rh–Rh bond, expect for $N = 13$. With the increase of cluster size, the adsorption of CO has less effect on the Rh–Rh bond of adsorbed CO molecule.

Generally speaking, face site adsorption occurs mainly in CO adsorbed on the clean surface of metal. For Rh_N clusters with large size, the adsorption stability of face site adsorption is stronger than those of bridge site adsorption and atop site adsorption. For $N = 16$, 18, 19, the adsorption site occurs on the triangle face.

Overall, the O atom does not directly bond with the Rh atom for three adsorption types. The adsorption of the CO molecule leads to the structural distortion and so lowers the symmetry of bare Rh cluster.

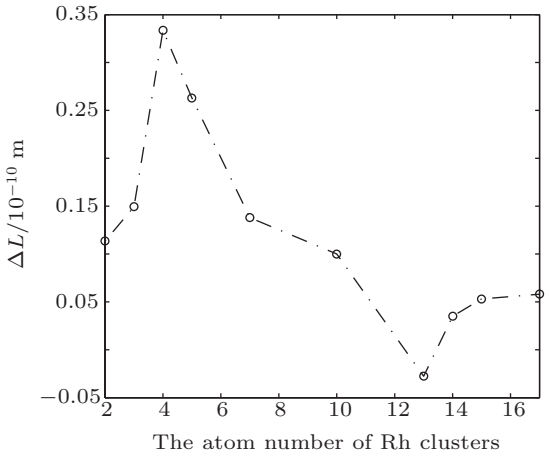


Fig. 4. Change in length of the Rh–Rh bond adsorbed by a CO molecule versus the atom number of Rh clusters for bridge-adsorption CO–Rh_N compounds.

3.2. C–O bond length, vibrational frequency and adsorption energy

The bond length and the vibrational frequency information about small molecule absorbed on the cluster can usually be used to evaluate the catalytic ability. The C–O and Rh–C bond lengths in the CO–Rh_N compounds are listed in Table 1, each as a function of cluster size. The frequency information about the C–O bond is shown in Fig. 5. The C–O bond length is elongated by 2.3%–5.5%, compared with that of the free CO molecule with bond length 1.142 Å. The length of C–O bond in the CO–Rh compound with atop site adsorption type is the smallest among three adsorption types. The result indicates that the adsorption ability of atop site adsorption is weaker than those of the two other adsorption types. The vibrational frequency information is identified based on a careful analysis of the eigenmode obtained through frequency calculations. The results of vibrational frequency suggest that redshifts of adsorption band occur under the interaction of Rh atoms. The C–O vibrational frequency varies in a range of 1700.81 cm^{-1}–1980.12 cm^{-1}, which is smaller than that of the free CO molecule, 2126.18 cm^{-1}. For the adsorption of CO in bridge position, the redshifts are about between 308.59 cm^{-1} and 424.37 cm^{-1}. While the data of the redshifts vary from 145.43 cm^{-1} to 179.01 cm^{-1} for the adsorption of CO in atop position. The large C–O bond length values correspond to small vibrational frequency data. For example, the C–O bond length for $N = 4$ is longest in Table 1, its corresponding vibrational frequency is smallest, located on bottom in Fig. 5. It is explained that the increased antibonding $2\pi^*$ is consistent with greater heats of adsorption and red-shift of the vibrational energy, because increasing occupation of this orbital weakens the C–O bond, which enlarges the C–O bond distance and the stretch vibration shifts toward lower frequencies.[41]

Table 1. The values of E_{ads} of CO–Rh_N complexes, Mulliken charge transfer distribution (Q) of the C, O and the nearest neighbouring Rh atom to C atom in CO–Rh_N complexes, and partial bond length (L), including C–O and Rh–C representing the shortest Rh–C bond length.

N	L_{Rh-C}/Å	L_{C-O}/Å	E_{ads}/eV	Q_{Rh}/e	Q_C/e	Q_O/e
2	1.950	1.192	3.022	–0.112	0.468	–0.243
3	1.936	1.198	2.844	–0.127	0.535	–0.276
4	1.927	1.206	2.631	–0.081	0.565	–0.306
5	1.946	1.202	2.383	–0.090	0.533	–0.286
6	1.855	1.171	2.384	–0.244	0.403	–0.208
7	1.956	1.195	2.584	–0.155	0.477	–0.255
8	1.863	1.169	2.195	–0.222	0.430	–0.202
9	1.860	1.170	2.507	–0.258	0.411	–0.203
10	1.978	1.190	2.367	–0.095	0.460	–0.235
11	1.856	1.168	2.343	–0.280	0.420	–0.197
12	1.863	1.168	2.199	–0.236	0.438	–0.194
13	2.022	1.187	2.482	–0.097	0.397	–0.237
14	2.018	1.189	2.374	–0.095	0.419	–0.237
15	2.015	1.189	2.411	–0.068	0.411	–0.230
16	2.020	1.206	2.390	–0.035	0.387	–0.257
17	1.997	1.190	2.252	–0.235	0.435	–0.204
18	2.056	1.205	2.272	–0.053	0.382	–0.257
19	2.050	1.206	2.275	–0.053	0.382	–0.257

Normally, when molecules physically interact with a surface by van der Waals force, physisorption occurs and the adsorption energy of 0.2 eV is insufficient to break bonds. Therefore, the adsorbed molecules retain their identities. The chemisorption occurs when a molecule chemically bonds to a surface,

usually through a covalent bond. This energy of adsorption is approximately 2.0 eV. When CO molecule is adsorbed on bare Rh cluster, the adsorption energy is greater than 2.0 eV, chemisorption dominates the CO adsorption on bare Rh_N clusters. The C–O bond is elongated. The adsorption of CO molecule especially has an enormous effect on the structure of a bare Rh cluster for bridge site adsorption type.

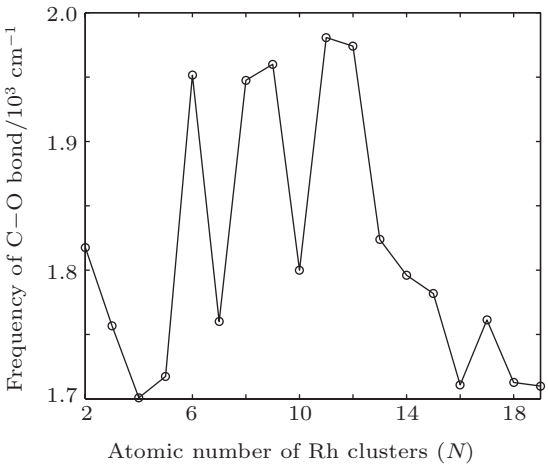


Fig. 5. C–O vibrational frequency in CO–Rh_N compounds versus atom number of Rh clusters.

The adsorption energy (E_{ads}) is often used to measure the capability of chemical reactivity of the cluster, which is defined as

$$E_{ads}(N) = E(Rh_N) + E(CO) - E(Rh_NCO), \quad (3)$$

where $E(*)$ values are the total energy of the relaxed Rh_N cluster, free CO molecule and CO–Rh_N compound, respectively. The E_{ads} is presented in Table 1 and plotted in Fig. 6 as a function of bare Rh cluster size. Obviously, the values of E_{ads} of $N = 8$, 12 are lower than those of other sizes. These results can be understood from their different adsorption sites, symmetries and stabilities of bare Rh clusters. For $N = 8$, 12, the ground-state structures are viewed as the atop site adsorption of CO molecule. The symmetry is O_h for bare Rh_8 and D_{4h} for bare Rh_{12}, respectively. The Rh_8 cluster and the Rh_{12} cluster are both more stable than their neighbouring clusters. Their corresponding CO–Rh_N complexes possess lower E_{ads} than other CO–Rh_N compounds.

However, the bond length and the vibrational frequency do not provide the whole picture of the adsorption energy. For the CO–Rh_6 compound with atop site adsorption, the change in bond length and vibrational frequency are particularly small, compared with those of free CO molecule, while it has relatively high adsorption energy.

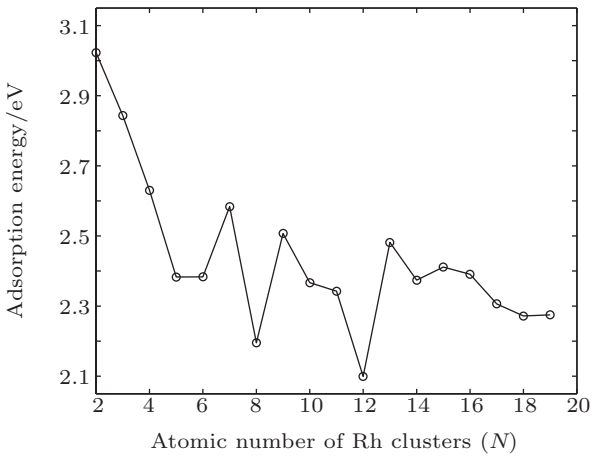


Fig. 6. The values E_{ads} of CO–Rn_N (N = 2–19) compounds versus atom number of Rh clusters.

3.3. Charge properties and electronic density

The charge transfer process plays an important role in the ground-state structure and adsorption strength. The charge transfer distribution (via Mulliken population analysis) among C, O, and Rh atoms are indicated in Table 1. The charge transfer is about 0.194 e–0.306 e between C and O atoms. While the O atom obtains only 0.096 e from C atom for free CO molecule. It is well known that the C–O bond is covalent bonding in free CO molecule. The less charge transfer indicates that there is a small polarity between C and O atoms. The charge transfer suggests the change in C–O bond length, and more charge transfer corresponds to a larger change in C–O bond length. With the increase of charge transfer, the ability of adsorption apparently strengthens. For example, the adsorption energy is 2.631 eV for CO–Rh_4 compound with a charge transfer of 0.306 e. It is found that the charge transfer between CO molecule and Rh clusters of atop site adsorption is smaller than that of bridge site adsorption expect for CO–Rh_{11} complex. For the face site adsorption, the charge transfer between C and O atom is about 0.257 e, and the charge transfer between CO molecule and Rh cluster is not apparent. The CO molecule donates charges to the Rh atom which is the nearest neighbouring to C atom. The charge transfer between C and Rh atoms is large, while the Rh–C bond length is small. For instance, the Rh atom neighbouring to C atom obtains 0.222 e and the Rh–C bond length is about 1.863 Å for CO–Rh_8. The value of charge transfer is 0.095 e between C

and Rh atoms for CO–Rh_{14} compound and the Rh–C bond length of CO–Rh_{14} is about 2.018 Å.

We show the electron densities of state (DOSs) in Fig. 7 including those of bare Rh_N clusters, CO–Rh_N compounds and CO in CO–Rh_N compounds ($N = 4$, 12, 14, 19). The DOS of the d orbital is particularly noticeable near 0 energy level and the d orbitals hybrid with s and p orbitals. The adsorption types of CO–Rh_4 and CO–Rh_{14} are both the bridge site adsorption, total DOS near 0 energy level suggests stronger interaction between CO molecule and Rh_4 cluster than that of CO–Rh_{14} compound. The E_{abs} of 2.631 eV for CO–Rh_4 compound is really larger than that of 2.374 eV for CO–Rh_{14} compound. Although the adsorption patterns are different, the DOS of adsorbed CO molecule is similar to those of CO–Rh_{12} with atop site adsorption, CO–Rh_{14} with bridge site adsorption, and CO–Rh_{19} with face site adsorption. The adsorption of CO molecules induces less effect on the DOS for bare Rh clusters with large size. Figure 6 indicates that the adsorption energy tends to be about 2.2 eV–2.3 eV with the increase of cluster size. We may further predict the adsorption energy tends to be constant value which is about equal to the adsorption energy data of CO molecules adsorbing on Rh (111) surface.

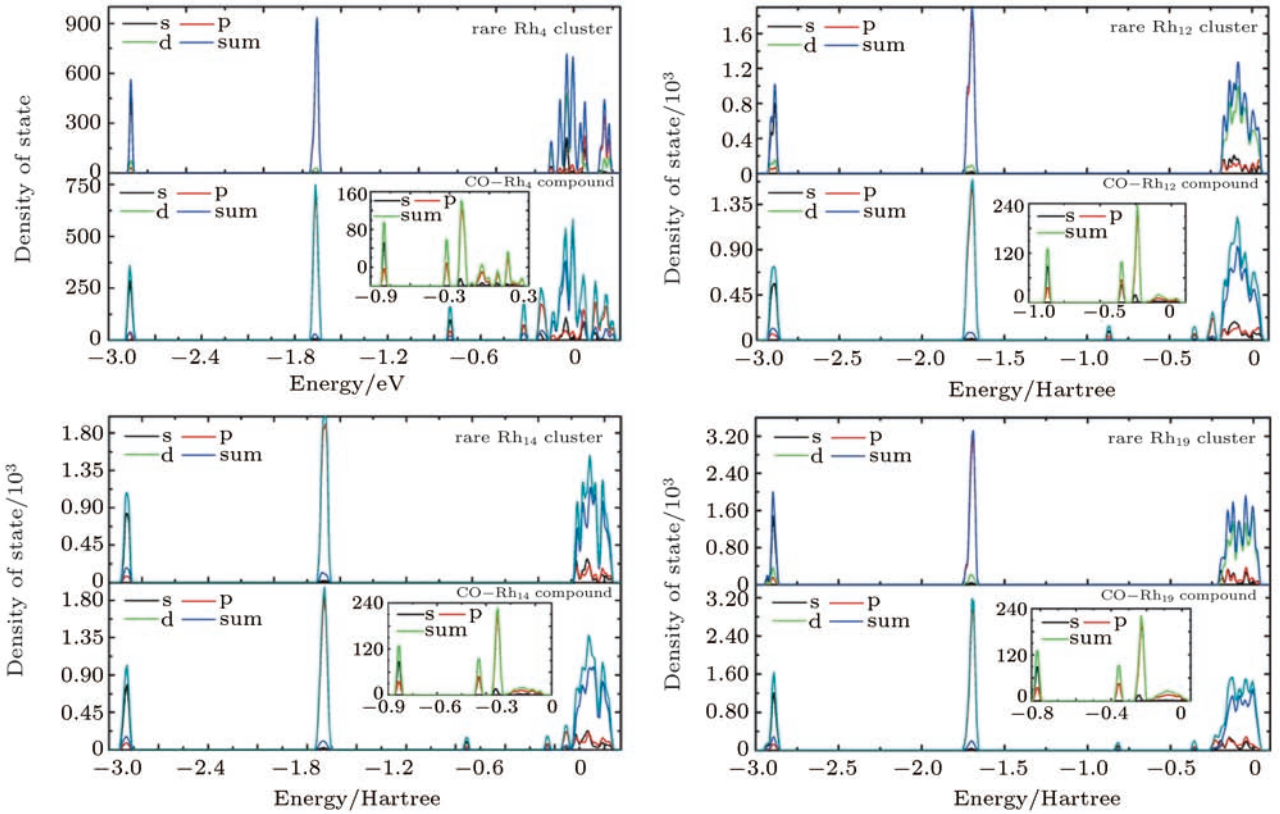


Fig. 7. (colour online) The DOSs of s, p and d orbitals, and total DOSs for bared Rh_N clusters and CO–Rh_N ($N = 4$, 8, 12, 19) compounds, with the insets displaying DOS of CO in the CO–Rh compounds, respectively.

4. Conclusion

The ground-state structures of bare Rh clusters, optimal adsorption sites, CO adsorption ability, and electronic properties of CO–Rh_N (N = 2–19) compounds are studied, using the generalized gradient approximation exchange–correlation potential method based on density functional theory. The structural growth model of bare Rh_N clusters transforms from double layers (N = 12–16) to three layers (N = 17–19). Three different adsorption types are the atop site adsorption for the sizes of N = 6, 8, 9, 11, 12, the bridge site adsorption for N = 2–5, 7, 10, 13–15, 17, and the face adsorption for N=16, 18, 19. The average binding energy and the second-order energy differences indicate that the stabilities of bare Rh_N clusters display odd–even oscillation. The adsorption strengths are predicted by the C–O bond length, the vibrational frequency of C–O bonding, the adsorption energy and the charge transfer between the CO and

the Rh clusters as well as electronic density of state. With the increase of Rh cluster size, the adsorption energy of CO adsorption on Rh_N cluster tends to be 2.2 eV–2.3 eV, which is 0.2 eV–0.3 eV larger than the theoretical data (about 2.0 eV) of CO molecule adsorbed on a clean Rh (111) surface.

References

[1] Fielicke A, Helden G V, Meijer G, Pedersen D B, Simard B and Rayner D M, 2006 *J. Chem. Phys.* **124** 194305

[2] Gruene P, Fielicke A, Meijer G and Rayner D M 2008 *Phys. Chem. Chem. Phys.* **10** 6144

[3] Lyon J T, Gruene P, Fielicke A, Meijer G and Rayner D M 2009 *J. Chem. Phys.* **131** 184706

[4] Fielicke A, Gruene P, Meijer G and Rayner D M 2009 *Surf. Sci.* **603** 1427

[5] Gutsev G L, Bauschlicher C W and Andrews L 2003 *J. Chem. Phys.* **119** 3681

[6] Wang Y and Gong X G 2006 *J. Chem. Phys.* **125** 124703

[7] Padilla-Campos L 2008 *J. Mol. Struct: THEOCHEM* **851** 15

[8] Tian F Y, Shen J and Wang Y X 2010 *J. Phys. Chem.* A **114** 1616

[9] Wang Y, Wang C and Wang S 2011 *Chin. Phys.* B **20** 036801

[10] Zhou M and Andrews L 1999 *J. Am. Chem. Soc.* **121** 9171

[11] Zhou M and Andrews L 1999 *J. Phys. Chem.* A **103** 7773

[12] Mineva T, Russo N and Freund H J 2001 *J. Phys. Chem.* A **105** 10723

[13] Swart I, Groot F M F, Weckhuysen B M, Rayner D M, Meijer G and Fielicke A 2008 *J. Am. Chem. Soc.* **130** 2126

[14] Fielicke A, Helden G V, Meijer G, Simard B, Dénommée S and Rayner D 2003 *J. Am. Chem. Soc.* **125** 11184

[15] Fielicke A, Helden G V, Meijer G, Simard B, Dénommée S and Rayner D 2004 *J. Phys. Chem.* B **108** 14591

[16] Cox A J, Louderback J G, Apsel S E and Bloomfield L A 1994 *Phys. Rev.* B **49** 12295

[17] Wang H, Haouari H, Craig R, Liu Y, Lombardi J R and Lindsay D M 1997 *J. Chem. Phys.* **106** 2101

[18] Adlhart C and Uggerud E 2005 *J. Chem. Phys.* **123** 214709

[19] Harding D, Ford M S, Walsh T R and Mackenzie S R 2007 *Phys. Chem. Chem. Phys.* **9** 2130

[20] Beyer M K and Knickelbein M B 2007 *J. Chem. Phys.* **126** 104301

[21] Harding D J, Walsh T R, Hamilton S M, Hopkins W S, Mackenzie S R, Gruene P, Haertelt M, Meijer G and Fielicke A 2010 *J. Chem. Phys.* **132** 011101

[22] Chien C H, Blaisten-Barojas E and Pederson M R 1998 *Phys. Rev.* A **58** 2196

[23] Chien C H, Blaisten-Barojas E and Pederson M R 2000 *J. Chem. Phys.* **112** 2301

[24] Harding D, Mackenzie S R and Walsh T R 2006 *J. Phys. Chem.* B **110** 18272

[25] Zhang W, Xiao L, Hirata Y, Pawluk T and Wang L 2004 *Chem. Phys. Lett.* **383** 67

[26] Bae Y C, Osanai H, Kumar V and Kawazoe Y 2004 *Phys. Rev.* B **70** 195413

[27] Bae Y C, Kumar V, Osanai H and Kawazoe Y 2005 *Phys. Rev.* B **72** 125427

[28] Chou J P, Chen H Y T, Hsing C R, Chang C M, Cheng C and Wei1 C M 2009 *Phys. Rev.* B **80** 165412

[29] Sun Y, Fournier R and Zhang M 2009 *Phys. Rev.* A **79** 043202

[30] Aguilera-Granja F, García-Fuente A and Vega A 2008 *Phys. Rev.* B **78** 134425

[31] Wang L and Johnson D 2007 *Phys. Rev.* B **75** 235405

[32] Nayak S K, Weber S E, Jena P, Wildberger K, Zeller R and Dederichs P H 1997 *Phys. Rev.* B **56** 14

[33] Yang J, Toigo F, Wang K and Zhang M 1994 *Phys. Rev.* B **50** 7173

[34] Dufour L 2001 *Int. J. Quantum Chem.* **85** 162

[35] DMOL is a density functional theory program distributed by Accelrys, Inc. B. Delley 1990 *J. Chem. Phys.* **92** 508; 2000 **113** 7756

[36] Perdew J P, Burke K and Ernzerhof M 1996 *Phys. Rev. Lett.* **77** 3865

[37] Delley B 2002 *Phys. Rev.* B **66** 155125

[38] Lide D R 1995 *CRC Handbook of Chemistry and Physics* 73rd edn. (Boca Raton: CRC Press) pp. 9–15

[39] *NIST Standard Reference Database* 69 March 2003 Release: NIST Chemistry WebBook

[40] Mainardi D S and Balbuena P B 2003 *J. Phys. Chem.* A **107** 10370

[41] Yoon B, Häkkinen H, Landman U, Wörz, A S, Antonietti J M, Abbet S, Judai K and Heiz U 2005 *Science* **307** 403